Performance comparison between two different injector configurations in a hybrid rocket

C. Carmicino *, A. Russo Sorge

University of Naples "Federico II", Department of Space Science and Engineering "L.G. Napolitano", P. le Tecchio 80, 80125 Napoli, Italy

Received 30 January 2006; received in revised form 28 July 2006; accepted 4 August 2006

Available online 8 December 2006

Abstract

Mass flux and pressure are usually considered the main parameters affecting the fuel regression rate in hybrid rockets, whereas the influence of the oxidiser injector is often neglected. Nevertheless, in some specific configurations, even in conventional hybrids, a noticeable dependence of regression rate on oxidiser injection modes has been found. Gaseous oxygen and polyethylene fuel cylindrical grains were burned. Results from the firing tests conducted with a conical axial injector of the oxidiser are discussed. That configuration provides highly stable combustion so it is considered very interesting and, hence, deserving of an in-depth analysis. A comparison to the results obtained with a radial injector is drawn in terms of average and instantaneous regression rate, fuel consumption profiles, and combustion efficiency and stability. The radial injector, at the same mass flux and pressure, produces lower regression rate, high pressure oscillations and worse combustion efficiency.
© 2006 Elsevier Masson SAS. All rights reserved.

Resumi

I fattori che generalmente si ritiene abbiano maggiore influenza sulla velocità di regressione del combustibile in un endoreattore a propellenti ibridi sono il flusso di massa e la pressione in camera, mentre spesso si trascura l'effetto che ha l'iniezione dell'ossidante. Nonostante ciò, in talune configurazioni, anche negli ibridi convenzionali, è stata riscontrata una dipendenza significativa della velocità di regressione dalle caratteristiche di iniezione dell'ossidante. Ossigeno gassoso e grani cilindrici di polietilene sono i propellenti utilizzati in questo lavoro. I risultati delle prove statiche del motore condotte con un iniettore conico assiale sono discussi in questa sede. Una tale configurazione genera un processo di combustione molto stabile cosicché se ne ritiene di grande interesse l'analisi sperimentale. Un confronto con i risultati derivanti dall'utilizzo di un iniettore radiale è affrontato in termini di velocità di regressione media ed istantanea, uniformità del consumo ed efficienza e stabilità di combustione. L'iniettore radiale, a parità di flusso di massa e pressione, produce velocità di regressione inferiori, elevate oscillazioni di pressione ed una peggiore efficienza di combustione.
© 2006 Elsevier Masson SAS. All rights reserved.

Keywords: Hybrid rocket; Oxidiser injector; Ultrasound pulse-echo technique

Parole chiavi: Razzo ibrido; Iniettore dell'ossidante; Ultrasuoni

1. Introduction

As widely discussed in the literature, the hybrid rocket engine provides several well-defined advantages over both solid-propellant and liquid-propellant motors. Thrust tailoring and stop-restart capability, its intrinsic safety, simplicity and lower cost, the latter deriving also from reduced manufacturing tol-

erances, can be reminded among the hybrid's most attractive features which often render hybrid motor the rocket chosen by both universities and rocket amateurs.

The fuel grain regression rate is the fundamental parameter required by designers for assessing the hybrid internal ballistics. Nevertheless, even though hybrids are known from more than 70 years, the regression process is still far from being completely modelled and the performance prediction has usually been based on simplified methods and correlations. The two main areas that have traditionally not been adequately ad-

---

Nomenclature

D	instantaneous local port diameter		p	chamber pressure
D_0	initial port diameter		$\dot{r}$	regression rate
D_2	final local port diameter		$\bar{\bar{r}}$	time and space averaged regression rate
G	total mass flux		t	time
$\overline{G}_{\text{ox}}$	average oxidiser mass flux		x	axial abscissa on the grain
L	grain length		ε	mixing efficiency index
O/F	average oxidizer mass to average fuel mass ratio		η	c^* efficiency, ratio between the actual and theoretical c^*
$(O/F)_{\text{st}}$	stoichiometric mixture ratio			

---

dressed in the open literature are the effect of oxidiser injector design and geometry on regression rate characteristics and the scaling effects. In fact, for the sake of simplicity, on the basis that the regression rate is controlled by heat transfer to the solid wall, it is often assumed that, in the classical hybrids, the regression rate can be expressed by a power function of the oxidiser mass flux. The exponent of this relationship is found to vary a lot depending on the propellant formulation and on the specific engine configuration, and values between 0.4 and 0.9 are generally observed. Other dimensional correlations accounting for grain diameter and/or length, and chamber pressure, appear as variants of this mostly used semi-empirical regression rate law. Thus, no universal formulae exist to calculate the fuel consumption of a given hybrid motor. Actually, if one tries to extrapolate the data from an experimental apparatus to another, the usage of a given relation can lead to considerable disagreements between the expected and measured regression rates. One reason for this discrepancy, apart from the possibly different motor scales, can be searched in the influence of the oxidiser injection characteristics upon the combustor inlet conditions. Indeed, changing the injector configuration, the fuel regression and, more in general, the entire motor behaviour will be influenced.

Just to give an example, let us consider the regression rate equation developed by Korting et al. [6] through experimental results derived from a hybrid rocket firing gaseous oxygen and polyethylene fuel:

$$\bar{\bar{r}} = 0.063 G^{0.36} p^{0.22} \tag{1}$$

where the units used are mm/s for the mean regression rate, $\bar{\bar{r}}$, kg/m^2 s for the mass flux, G, and MPa for the chamber pressure, p. This equation, assuming $G = 50$ kg/m^2 s and $p = 2$ MPa, predicts that the regression rate would be 0.25 mm/s. At the same mass flux and pressure, this result really underestimates by 100% the fuel regression rate (0.5 mm/s) measured by the authors in Ref. [3]. Notice that this comparison has been made with the same propellants, and that both the grain inner diameter and length are approximately equal as well. Interestingly, the authors [3] found a correlation in the same form as that previously mentioned (Eq. (1)) with practically the same exponents of both mass flux and pressure. Hence, the same low dependence of regression rate upon the mass flux was determined but the regression rates are definitely different in magnitude. This argument demonstrates that any other factors must affect the fuel regression.

This paper reports a summary of a complete comparison between the results ensuing from the combustion experiments in cylindrical port hybrid grains subjected to axial and radial injection of gaseous oxygen. Average fuel consumption and local regression rate measurements, the latter performed with the ultrasound pulse-echo technique, were used for this purpose. A conical subsonic nozzle and a radial injector were selected to generate different conditions for the oxidiser at the entrance of the fuel port. The axial injector, in particular, is considered interesting because of its relatively easy design and the remarkable quality that, as demonstrated also in Ref. [2], it produces a stable combustion with no substantial pressure oscillations, due to the large hot gas recirculation zone inside the combustion port. In order to take advantage of this aspect, it is necessary to investigate the regression rate behaviour under the flow field generated by this injector, then most of the tests were carried out on this configuration.

2. Apparatus and procedure for experimental investigations

A scheme of the lab-scaled motor is reported in Fig. 1. However, more details can be found in Ref. [10]. Gaseous oxygen is supplied at mass flow rates up to 0.25 kg/s that are measured with a venturi tube. The oxygen is injected into the chamber either through a radial injector or an axial injector. In the latter case, a converging nozzle is employed whose exit diameter is 8 mm. The Mach number at the axial injector exit section is at most 0.39. Nitrogen is purged into the chamber by a switch valve (oxygen or nitrogen) for the burn out and in case of an accident. The ignition was accomplished using a pyrotechnic igniter.

Cylindrical one-port high density polyethylene fuel grains, 560 mm long, were tested. Four initial inner diameters, 16, 25, 50 and 75 mm, were selected in order to explore a wide range of mass fluxes, grain length to diameter ratios and injector to grain port diameters ratio. Two chambers were set up ahead and aft of the grain; the first one, made by Teflon®, to shift toward the fore end of the grain the strong recirculation region caused by the oxygen injection in an attempt to increase the overall regression rates; the second one, made by stainless steel covered with thermal protections, to promote further gas mixing, thereby improving the combustion efficiency.
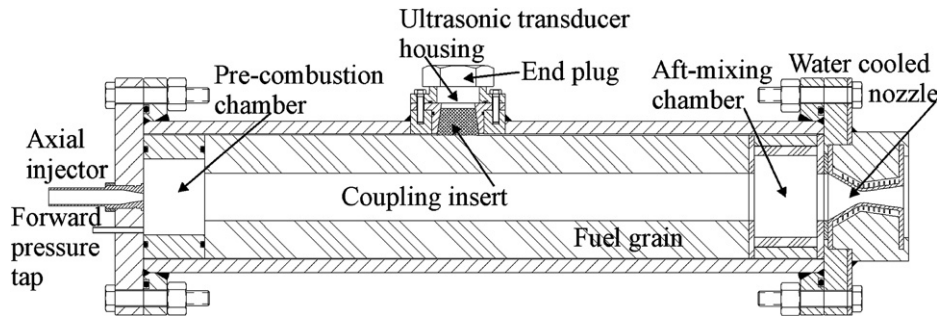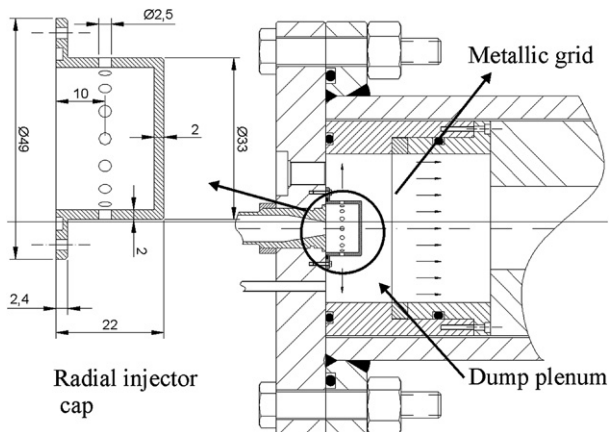
Fig. 1. Scheme of the lab-scale hybrid motor.

Fig. 2. Motor forward-end section: radial injector and dump plenum (dimensions are in mm).

A second series of tests was carried out using a configuration with a radial injector feeding oxygen into a dump plenum (made by stainless steel). The oxygen injector assembly, shown in Fig. 2, produces a high speed radial flow of oxygen via 16 equally spaced 2.5 mm diameter orifices around the periphery of the injector cap. This injection technique should prevent the high recirculation spanning the entrance of the grain which, instead, is yielded by the axial injector [2]. In addition, some tests were performed with a metallic grid placed in the dump plenum for further reducing the vorticity produced in order to provide a relatively more uniform flow at the combustion port entry.

A water cooled De Laval nozzle with 16 mm throat diameter and 2.44 area ratio, made of copper alloy, ensures long time tests with no throat erosion.

Chamber pressure is measured by two capacitive transducers, set up in the pre-chamber and in the mixing chamber. All of the signals are sampled at 100 Hz, recorded and processed by the software that also controls the system.

The regression rate over time is measured by means of an ultrasounds equipment. One ultrasonic transducer, located around the middle of the chamber, is employed in order to obtain the time evolution of the local grain thickness and, in turn, the regression rate in that point.

The ultrasonic transducer is a Panametrics Videoscan V114-SB of 3/4 in nominal diameter and 1 MHz central frequency. The signals emitted by the transducer are generated and amplified by a pulser-receiver device (Panametrics model 5072PR), acquired by an oscilloscope and processed with an oscillo-

scope proper function which computes, with a frequency of 10 Hz, the time lapse between the trigger event (transmitted wave) and the first zero-crossing point with positive slope of the echo waveform corresponding to the inner surface of the grain. This frequency is limited by the oscilloscope performance, anyway, since the fuel may have a regression rate of 1 mm/s or lower, for quasi-steady applications it seems fairly good. Recently a new technique has been developed for the ultrasound measurements: the ultrasound waveforms are sampled by a National Instruments 5112 PCI digitiser at 100 MHz frequency and with a pulse repetition frequency equal to 100 Hz (ten times higher than the value limited by the oscilloscope). Then, the ultrasound signals are analysed by means of a cross correlation technique in order to compute the time delay between two appropriate echoes. This method has been applied only to process the data from the tests performed with the radial injector configuration. The instantaneous grain thickness was calculated from the waves propagation time considering the wave speed in the fuel equal to that measured in reference conditions [3,13]. The thickness data were filtered with a Gaussian low-pass filter having a cut-off frequency of 3 Hz, and a derivative central formula was applied for the regression rate calculation. The time-space-averaged regression rate was simply calculated from the fuel mass loss, and the average mass flux was referred to the average port diameter.

3. Analysis of results

The experimental test conditions and some of calculated mean parameters relative to the radial injector are listed in Table 1. An analogous test data sheet for the axial injector motor is given in Ref. [3].

Time and spatially averaged regression rates measured in this study are depicted in Fig. 3 as a function of the total mass flux for both axial and radial injection configurations, together with those reported in Refs. [6,9]. The tests in Ref. [9] were conducted with polyethylene fuel but in a ram-rocket motor where the fuel grain was loaded downstream of the gas generator's solid propellant, so it was exposed to high temperature (about 2800 K) combustion gas. All of the tests presented here were carried out with chamber pressures in the rage of 0.4–2.5 MPa. These two sets of data were chosen from the available literature because they have been obtained from laboratory rockets of similar sizes and operating conditions, and yield regression rates which, though different, are reasonably compa-

Table 1
Radial injector tests table

| Test	D_0 (mm)	$\dot{m}_{ox}$ (kg/s)	p (atm)	$\overline{G}_{ox}$ (kg/m² s)	G (kg/m² s)	O/F	$\bar{\dot{r}}$ (mm/s)	η
Radial injector								
1-R	50	0.21	18.51	79.51	97.96	4.31	0.52	0.853
2-R	67	0.16	13.52	38.02	44.45	5.91	0.23	0.898
3-R	50	0.16	14.12	48.74	57.55	5.53	0.28	0.899
4-R	25	0.15	13.33	77.99	93.50	5.03	0.38	0.920
5-R	50	0.15	12.10	47.31	55.52	5.76	0.25	0.886
6-R	25	0.14	13.48	103.1	124.50	4.82	0.44	0.945
7-R	75	0.14	11.17	28.95	33.6	6.26	0.18	0.885
8-R	52	0.14	12.86	54.40	65.12	5.07	0.31	0.919
9-R	16	0.16	16.45	119.13	150.30	3.82	0.62	0.931
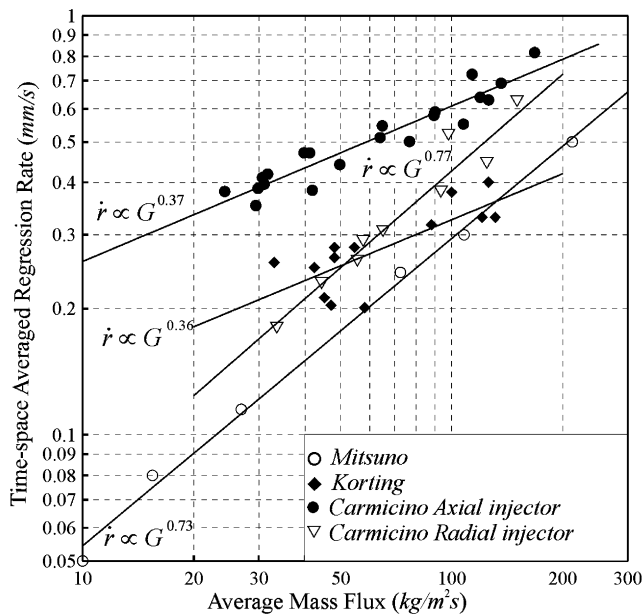
Fig. 3. Comparison of average regression rates.

rable. In Ref. [3] some data obtained by Lengellé et al. [7] were also considered but they have been discarded here since they show either too much lower regression or very high mass fluxes (1000–3000 kg/m²s).

Apart from the fact that the data in the literature [6,9] themselves reveal diverse mass flux dependence and values from each other (about which nothing can be said for the lack of precise information), the focal aspect to be noted in Fig. 3 is that, at the same mass flux and almost the same pressure levels, current fuel regression rate in the axial injection motor differently behaves in terms of both mass flux dependence and magnitude compared to the radial injector motor and to the data from Mitsuno [9] (lowest regression rates). In comparison to the regression rates measured by Korting [6], instead, the latter are lower as well but show a similar mass flux trend, as mentioned earlier. In fact, present axial-injection results indicate higher regression rates (up to at least 2.5 times faster than those in the literature, if compared with Ref. [6], or even more if compared with Ref. [9] whence 3.3 times faster regression is achieved) and lower influence of the mass flux itself, as demonstrated by the value of the power law exponent $n = 0.37$ against 0.73 from Ref. [9]

and 0.77 corresponding to the radial injector. Notice that the latter exponents are very close to 0.8 which is the value theoretically predicted based on a turbulent flow over a flat plate [8]. It should be observed that the regression rate increase in the hybrid rocket with the axial injector is more significant at low mass flux and tends to disappear at relatively high mass fluxes. In the present experimental conditions, 200 kg/m² s may be inferred as a limit value of mass flux whereby axial and radial injection motors will have nearly the same regression rates.

The reason for the different regression rate performance asserted here consists in the way the gaseous oxidiser is fed into the port. In fact, with regard to the experimental devices used within the works of Korting [6] and Mitsuno [9], in both of them there is no nozzle but an injection chamber that distributes, more or less uniformly, the oxidiser at the fuel port inlet. The latter circumstance is also met with the radial injector which presumably gives rise to a flow field where the axial component of velocity at the entrance of the grain is nearly constant over the radius. Therefore, average regression rates achieved by means of that motor configuration fall on the experimental data from Korting [6], except for the point at $G \sim 100$ kg/m² s (Fig. 3) which was affected by large pressure oscillations as will be discussed later.

Actually, by injecting oxygen with the conical nozzle, a flow recirculation zone is generated, which leads to a non uniform convective heat transfer distribution such that the wall heat flux and, thus, the regression rate rise from the zone downstream of the pre-chamber attaining a maximum at the jet impingement region, and, farther downstream, gradually decrease along the combustor axis.

An investigation into the port shape after burnout shows fuel consumption profiles consistent with the regression rate distribution just described (Fig. 4).

All of the curves in Figs. 4a and 4b ($D_0 = 75, 50$ mm) peak at an axial location that, in almost all of the cases, moves downstream as more fuel is burned. Different profiles are, instead, displayed in Figs. 4c and 4d ($D_0 = 25, 16$ mm) by the curves relative to Tests 1, 10, 19 and Tests 5 and 18. Fig 4 also depicts the estimated oxidiser jet diameter, plotted by assuming a divergence angle varying between 6° and 8°, which is typical of a free jet [1]. The comparison between the jet pattern and the port diameter profiles clearly suggests that the maximum regression rate falls in the region where the oxygen jet impinges on the grain's surface and, as a result, the maximum convective heat transfer is expected. Note that, as stated in Ref. [11], the turbulent Reynolds stress in the radial direction of a confined jet is much higher than those measured in a fully developed pipe flow and, furthermore, this turbulence is increased markedly in the presence of recirculation. Beyond the centre of the recirculation eddy, the intensity grows up rapidly to very large values so that more efficient heat transfer is likely. From these features one can see the effectiveness of a nozzle as an injector. The flow acceleration through the nozzle, indeed, generates higher axial velocity and vorticity in the port.

In the case of grains with 25 mm and 16 mm initial diameter, this behaviour appears not so marked possibly because of the small fraction of the port affected by the phenomenon of
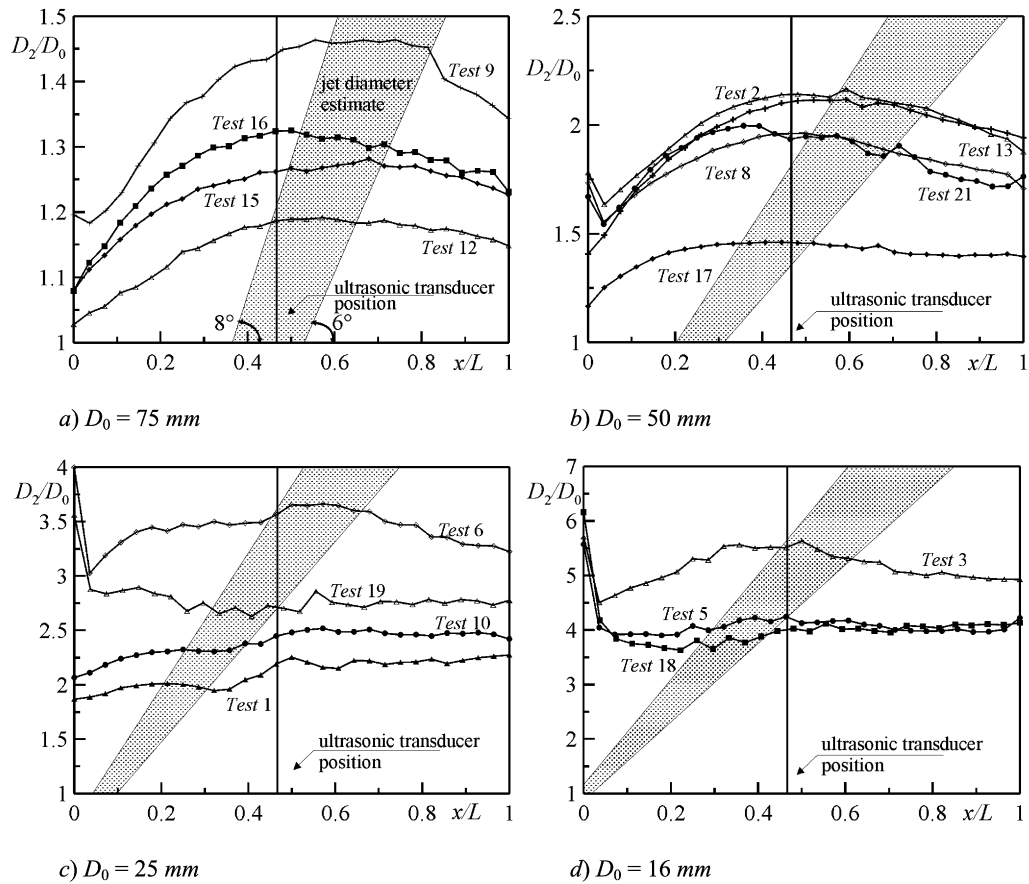
Fig. 4. After burn port diameter profiles (axial injector).

jet impingement. Indeed, also in this case, when larger diameters are reached (that is bigger amount of fuel is burned off), i.e. Test 6 for $D_0 = 25$ mm and Test 3 for $D_0 = 16$ mm, the situation turns quite similar. It is worth noting that this consumption profiles are typical of solid fuel ramjets where a rearward facing step is placed at the air inlet as flame holding [12]. There, combustion occurring in the mixing region preheats oxygen and gaseous fuel available to the leading edge of the diffusion flame increasing the local flame speed beyond the local flow speed, so establishing a stable combustion.

Looking at the instantaneous regression rates plotted versus the local instantaneous grain diameter (Fig. 5) supports the existence of a strong injection influence on the fuel consumption rate in that they reflect the heat transfer variations consequent on the dynamics of the jet impingement inside the port enlarging over time.

Relative to the case when $D_0 = 50$ mm, by qualitatively matching the corresponding data in Figs. 4b and 5a, one sees that the test conditions are such that, during the firing, oxygen impacts on the grain at the ultrasonic transducer location. This makes the local regression rate to appear increasing or nearly constant. Substantially different behaviour happens for $D_0 = 25$ mm (Figs. 4c and 5b): the regression rate exhibits a decreasing trend because the region of impingement lies upstream of the transducer except for Test 6 in which, actually, the regression rate begins to increase when $D/D_0 \cong 2.4$. Test 7 shows similar trend so, although the lack of post-firing port di-

ameter profile, the occurrence of an analogous situation can be supposed. The comparison with the inner profile of grains fired using the radial injector and the dump plenum allows us to confirm what pointed out earlier. In accordance with the curves in Fig. 6, for large initial port diameters the fuel consumption distribution is fairly uniform and similar to the ones in Figs. 4c and 4d ($D_0 = 25, 16$ mm) where the port diameter to injector diameter ratio is so small as to reduce the recirculation region extent.

Less uniform consumption is displayed by the port shape of Test 4-R (Fig. 6) for which the initial inner diameter is $D_0 = 25$ mm. This may be explained by considering that, a vena contracta effect, due to the large sudden contraction the gas undergoes as it moves from the dump plenum towards the combustion port, should be present. With the radial injector also the instantaneous regression rate changes as we expect from the average values in Fig. 3; indeed, as shown in Fig. 7 where oxidiser mass flux and chamber pressure versus time are reported, the mean trend of regression rate nearly follows that of the mass flux in contrast to the trends displayed in Fig. 5. Only Test 1 and Test 10 in that figure ($D_0 = 25$ mm) can be supposed to have a similar behaviour. For these tests, in fact, the injector effect is almost evanescent (see Fig. 4c).

Fig. 7 additionally shows the oscillatory behaviour of the chamber pressure which is definitely absent in all of the tests with the axial injector motor. Hence, as expected from the literature [2], the radial injection motor produced unstable com-
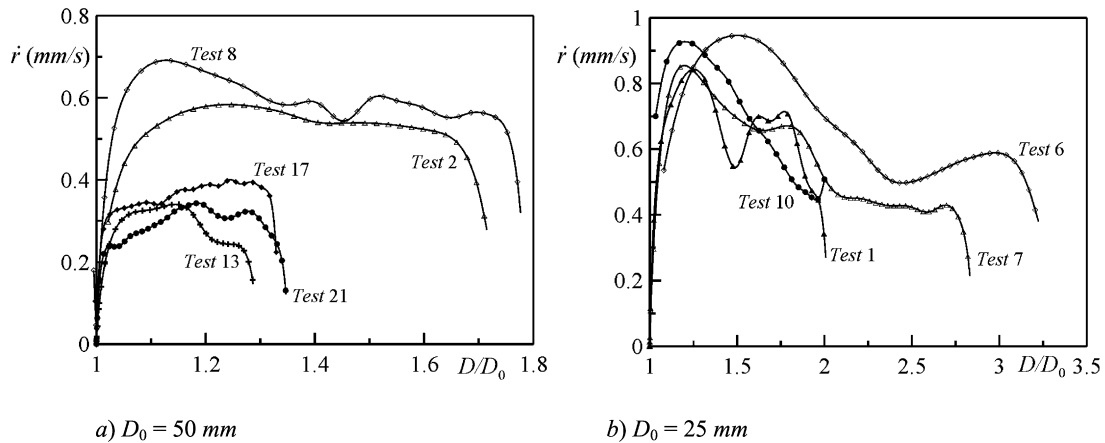
a) $D_0 = 50$ mm

b) $D_0 = 25$ mm

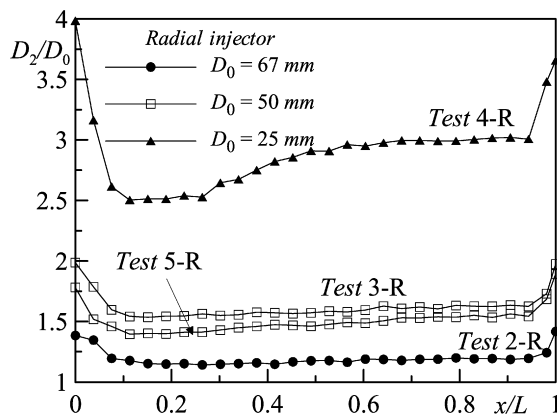Fig. 5. Local instantaneous regression rates (axial injector).

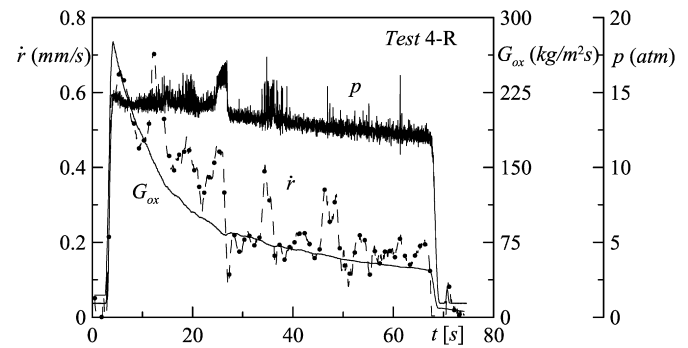Fig. 6. After burn port diameter profiles (radial injector).

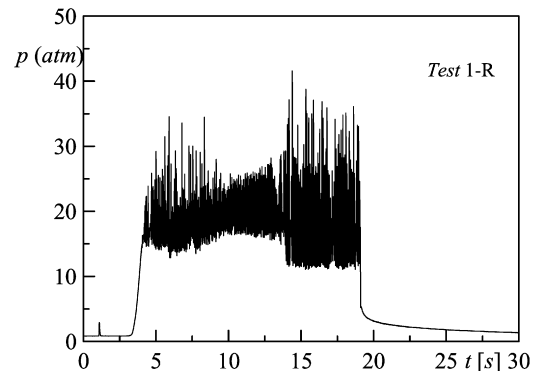Fig. 7. Local regression rate and oxygen mass flux, chamber pressure (radial injector).

Fig. 8. Chamber pressure (radial injector and metallic grid configuration).

bustion characterized by large amplitude pressure oscillations, on the order of 5 atm peak to peak, which occur together with enhanced fuel regression rate as demonstrated by the peaks roughly corresponding to the high pressure oscillations onset. The regression rate sharp increase occurring during pressure oscillation periods has been also documented by Dijkstra [4] and is strikingly evident in the first test performed with the radial injector cap, the dump plenum and the metallic grid (see Fig. 2). The average regression rate obtained in this test (Test 1-R) is much higher than one would expect at the corresponding mass flux ($G \sim 100$ kg/m^2 s in Fig. 3, as previously noted) and the relative pressure trace is shown in Fig. 8. As indicated by the pressure-time plot, the oscillations amplitude worsened as compared to Test 4-R in Fig. 7, reaching a peak-to-peak value close to 25 atm, even higher than the average pressure of 18.5 atm. This large oscillation was, to some extent, expected since the metallic grid should reduce the flow recirculation and thus the propellant mixing stabilizing the flame at the port inlet. Anyway, pressure oscillation was probably heightened by a coupling between the combustor dynamics and the oxidiser delivery system that is not isolated by any sonic choke. An in-depth study on this matter is planned for the next future.

Finally, it is very interesting to observe the combustion efficiency achieved by the axial and the radial injection configurations. Here the efficiency was defined as the ratio between the experimentally measured characteristic exhaust velocity to the theoretical one, the latter computed with the CEA chemical equilibrium code [5] at the effective mean pressure and mixture ratio.

As it is shown in Fig. 9a, most of the data from the axial injection motor correspond to efficiency around 95% at fuel rich mixture ratios, while the radial injection motor has lower efficiency with oxidiser rich mixture. This issue is believed to be due again to the recirculation zone present in the axial injection motor that promotes a mixing of oxidiser and fuel in the forward-end of the combustor port. This seems confirmed by the second diagram in Fig. 9b where the combustion efficiency
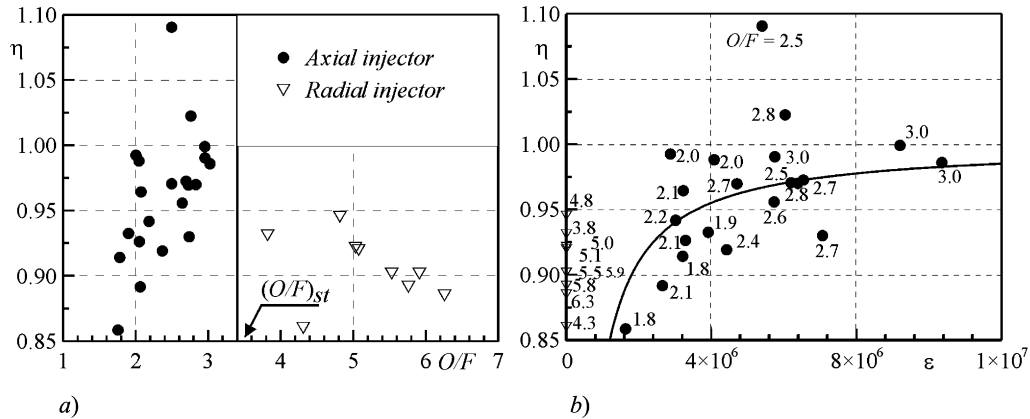
Fig. 9. Combustion efficiency.

was plotted versus the product of the oxidiser jet Reynolds number and the recirculation length to grain average diameter. This parameter, ε, may be qualitatively assumed as an index of the mixing efficiency since it is representative of both the jet eddy diffusivity and the mixing area but, of course, it was introduced just for a rough analysis. In this diagram the points from the radial injection motor were positioned at the origin ($\varepsilon = 0$) because the extent of the mixing region was ideally considered to be zero. It can be noticed that as the mixing efficiency increases the combustion efficiency increases as well.

4. Conclusions

Injector effects are conceived one of the most important aspects of hybrid combustor design, in fact, they can significantly affect the overall behaviour of the motor in terms of such important characteristics as the fuel consumption rate and uniformity, the combustion efficiency and the combustion stability. Since these effects may easily overshadow classical ballistic model calculations, there is a real need to investigate into the injector influence with the aim of developing reliable tools for performance prediction.

This paper dealt with the results of the static engine firings of a hybrid rocket where gaseous oxygen was supplied into axial-symmetric polyethylene cylindrical grains through two different injector configurations. An axial conical subsonic nozzle and a radial injector were tested for generating absolutely distinct oxidiser entrance conditions.

Average regression rates coming from the axial injector motor exhibited higher values and weaker mass flux dependence. This topic, in conjunction with the higher combustion stability and efficiency renders this configuration particularly attractive. The fuel consumption irregularity, however, has to be better studied in order to reduce the unburned fuel and, at the same time, try to raise the regression rate for motor applications that do not involve the highest thrusts.

References

[1] G.N. Abramovich, The Theory of Turbulent Jets, Massachusetts Institute of Technology, 1963, pp. 3–17.

[2] T.A. Boardman, D.H. Brinton, R.L. Carpenter, T.F. Zoladz, An experimental investigation of pressure oscillations and their suppression in subscale hybrid rocket motors, AIAA Paper 95-2689, July 1995.

[3] C. Carmicino, A. Russo Sorge, Role of injection in hybrid rockets regression rate behavior, Journal of Propulsion and Power 21 (4) (2005) 606–612.

[4] F. Dijkstra, P.A.O.G. Korting, R. van der Berg, Ultrasonic regression rate measurement in solid fuel ramjets, AIAA Paper 90-1963, 1990.

[5] S. Gordon, B.J. McBride, Computer program of complex chemical equilibrium compositions and applications, NASA Reference Publication 1311, 1994.

[6] P.A.O.G. Korting, H.F.R. Schöyer, Y.M. Timnat, Advanced hybrid rocket motor experiments, Acta Astronautica 15 (2) (1987) 97–104.

[7] G. Lengellé, B. Fourest, J.C. Godon, C. Guin, Condensed phase behavior and ablation rate of fuels for hybrid propulsion, AIAA Paper 93-2413, 1993.

[8] G.A. Marxman, M. Gilbert, Turbulent boundary layer combustion in the hybrid rocket, in: Ninth International Symposium on Combustion, Academic Press, New York, 1963, pp. 371–383.

[9] M. Mitsuno, T. Kuwabara, K. Kosaka, K. Shirota, Experimental study on solid fuel ram rocket, in: 31st IAF Conference, September 1980.

[10] A. Russo Sorge, The state of art of hybrid propulsion research in Italy, in: Proceedings of the 8th International Workshop on Combustion and Propulsion, Pozzuoli, June 2002, pp. 09-1–09-7.

[11] J.A. Schetz, Injection and mixing in turbulent flow, in: M. Summerfield (Ed.), Progress in Astronautics and Aeronautics, vol. 68, AIAA, New York, 1980, pp. 85–92.

[12] G. Shulte, Fuel regression and flame stabilization studies of solid-fuel ramjets, Journal of Propulsion and Power 2 (4) (1986) 301–304.

[13] J.C. Traineau, P. Kuentzmann, Ultrasonic measurements of solid propellant burning rates in nozzleless rocket motors, Journal of Propulsion and Power 2 (3) (1986) 215–222.